Wang et al. BMC Neurology (2021) 21:195
https://doi.org/10.1186/s12883-021-02224-6

BMC Neurology

RESEARCH Open Access

BRAF$^{non\text{-}V600E}$ more frequently co-occurs with *IDH1/2* mutations in adult patients with gliomas than in patients harboring *BRAF*^{V600E} but without a survival advantage

Wei Wang[1], Maode Wang[1], Haitao Jiang[1], Tuo Wang[1] and Rong Da[2*]

Abstract

Background: The effects of *BRAF*$^{non\text{-}V600E}$ and *BRAF*^{V600E} on the outcomes and the molecular characteristics of adult glioma patients are unknown and need to be explored, although *BRAF*^{V600E} has been extensively studied in pediatric glioma.

Methods: Co-occurring mutations and copy number alterations of associated genes in the MAPK and p53 pathways were investigated using data from The Cancer Genome Atlas (TCGA) public database retrieved by cBioPortal. The prognosis of available adult glioma cohorts with *BRAF*^{V600E} and *BRAF*$^{non\text{-}V600E}$ mutations were also investigated.

Results: Ninety patients with *BRAF*^{V600E} or *BRAF*$^{non\text{-}V600E}$ were enrolled in this study, and data from 52 nonredundant patients were investigated. Glioblastoma multiform was the most common cancer type, with *BRAF* $^{non\text{-}V600E}$ and *BRAF*^{V600E}. *TP53* (56.00% vs. 7.41%), *IDH1/2* (36.00% vs. 3.70%), and *ATRX* (32.00% vs. 7.41%) exhibited more mutations in *BRAF*$^{non\text{-}V600E}$ than in *BRAF*^{V600E}, and *TP53* was an independent risk factor (56.00% vs. 7.41%). Both *BRAF*$^{non\text{-}V600E}$ and *BRAF*^{V600E} frequently overlapped with *CDKN2A/2B* homozygous deletions (HDs), but there was no significant difference. Survival analysis showed no difference between the *BRAF* $^{non\text{-}V600E}$ and *BRAF*^{V600E} cohorts, even after excluding the survival benefit of *IDH1/2* mutations and considering the *BRAF*$^{non\text{-}V600E}$ mutations in the glycine-rich loop (G-loop) and in the activation segment. The estimated mean survival of patients with *BRAF*$^{non\text{-}V600E}$ & *IDH1/2*^{WT} with mutations in the G-loop groups was the shortest.

Conclusions: *BRAF*$^{non\text{-}V600E}$ exhibited a stronger association with *IDH1/2* mutations than *BRAF*^{V600E}, but no survival advantage was found.

Keywords: Adult patient with glioma, *BRAF*$^{non\text{-}V600E}$, *BRAF*^{V600E}, *IDH1/2*

* Correspondence: da_rong@xjtu.edu.cn
[2]Department of Clinical Laboratory, The First Affiliated Hospital of Xi'an Jiaotong University, No.277 Yanta West Road, Xi'an 710061, Shaanxi, China
Full list of author information is available at the end of the article

Background

BRAF (v-raf murine sarcoma viral oncogene homolog B1) is a serine-threonine kinase in the *Ras/Raf/*mitogen-activated protein kinase (MAPK) pathway [1, 2] that transduces mitogenic stimuli after the activation by growth factor receptors that are involved in cell survival, proliferation, and differentiation [3]. MAPK pathway activation is common in various neoplasms. Active *RAS* mutations have been detected in approximately 15% of malignant human tumors.

Compared with *ARAF* and *RAF1*, *BRAF* plays a critical role in kinase activity [4]. A previous study showed that *RAF1* is activated by *BRAF* through direct interactions between proteins and phosphorylation [5]. *BRAF* participates in the pathological mechanism of 7% of human neoplasms, especially in patients with melanoma and colorectal, thyroid, and lung cancer [6, 7]. The expression of *BRAF* is highly restrained [1, 8]. The high expression of *BRAF* in neural cells indicates that it is a vital MEK kinase in neuronal tissues [9, 10]. *BRAF* mutations are found in some central nervous system neoplasms. In pediatric low-grade gliomas (LGGs), these alterations correlate with oncogenic senescence, which may contribute to an improved prognosis [11]. The $BRAF^{V600E}$ mutation is rare in adult LGGs and glioblastomas and can only be found in 1 to 5% of samples [12, 13]. While *BRAF* activation contributes to tumor development and progression in the neural stem cells and progenitor cells of *Homo sapiens*, *BRAF* mutations are detected in adult diffuse gliomas and are associated with poor outcomes [14].

Most studies have focused on the $BRAF^{V600E}$ mutation, although more than 70 *BRAF* mutations have been reported to date. Mutations in *BRAF* at V600 can activate ERK, which plays a critical role in the G1/S transition by adjusting the expression of cyclin D, cyclin E, and p21Cip1 [15]. The $BRAF^{V600E}$ mutation is the most potent MAPK pathway activator, whereas $BRAF^{non\text{-}V600E}$ mutations are low-activity kinases that slightly stimulate the MAPK pathway [16]. However, these low-activity *BRAF* mutants could activate MAPK signaling in COS-1 cells to a high level by activating *RAF1* [16].

Isocitrate dehydrogenase (IDH) is a frequent mutation associated with a survival benefit in glioma patients and it has been defined as a molecular parameter to define the categories of brain tumors in the updated 2016 edition of the World Health Organization (WHO) Classification of Tumors of the Central Nervous System (CNS) [17]. *IDH1* and $BRAF^{V600E}$ mutations are associated with infiltrative gliomas or circumscribed gliomas and glioneuronal tumors, respectively [18, 19], and they are exclusive in most cases [20]. The exact effect of $BRAF^{non\text{-}V600E}$ and $BRAF^{V600E}$ on the prognosis of glioma patients and whether there are unique molecular characteristics in their MAPK and p53 pathways remain largely unknown.

In this study, co-occurring mutations and copy number alterations of 35 associated genes in the MAPK and p53 pathways were retrieved and investigated, and the prognosis of the available adult glioma cohorts with $BRAF^{V600E}$ and $BRAF^{non\text{-}V600E}$ were evaluated by using The Cancer Genome Atlas (TCGA) public database. We determined that $BRAF^{non\text{-}V600E}$ exhibited a stronger association with the *IDH1/2* mutation than $BRAF^{V600E}$, but no survival advantage was found.

Methods

Data collection and enrollment

All data were collected and generated from the TCGA public database using the TCGA data mining tool cBioPortal (https://www.cbioportal.org/) [21, 22]. We strictly followed the TCGA publication guidelines (https://www.cancer.gov/about-nci/organization/ccg/research/structural-genomics/tcga/using-tcga/citing-tcga). In multiple patient cohorts of all twenty available CNS/brain studies (6164 samples), the available data were queried, including the gene mutations, copy number alterations, mRNA expression, and protein expression data of patients with *BRAF* gene mutations. In each study, the mutations were selected for genomic profiles. Samples with mutation data were selected for the patient/case set and entered into three groups: (1) General: *Ras-Raf-MEK-ErK/JNK* signaling (26 genes), including *KRAS*, *HRAS*, *BRAF*, *RAF1*, *MAP 3 K1*, *MAP 3 K2*, *MAP 3 K3*, *MAP 3 K4*, *MAP 3 K5*, *MAP 2 K1*, *MAP 2 K2*, *MAP 2 K3*, *MAP 2 K4*, *MAP 2 K5*, *MAPK1*, *MAPK3*, *MAPK4*, *MAPK6*, *MAPK7*, *MAPK8*, *MAPK9*, *MAPK12*, *MAPK14*, *DAB2*, *RASSF1*, and *RAB25*; (2) General: p53 signaling (6 genes), including *TP53*, *MDM2*, *MDM4*, *CDKN2A*, *CDKN2B*, and *TP53BP1*; (3) Other frequently mutated genes, including *IDH1*, *IDH2*, and *ATRX*, were then submitted for query. Among the downloadable data files, the available data regarding the mutations, copy number alterations, mRNA expression, and protein expression were downloaded. In the type of genetic alterations across all samples, samples harboring the *BRAF* mutation were chosen. Data regarding mutations and copy number alterations on the summary page and the patient and sample data on the clinical data page were downloaded. All of the data were recorded in a chart for further analysis (Supplementary Dataset S1).

Major characteristics of the $BRAF^{V600E}$ and $BRAF^{non\text{-}V600E}$ cohorts using univariate logistic regression analysis

The enrolled populations were divided into $BRAF^{V600E}$ and $BRAF^{non\text{-}V600E}$ groups. The numbers and percentages of categorical variables were calculated. Their demographic characteristics, including sex, diagnosis age, cancer type, and overall survival status, were analyzed using univariate logistic regression analysis. The

odds ratios (ORs) and 95% confidence intervals (CIs) were estimated.

Co-occurring mutations of the *BRAF*^{V600E} and *BRAF*$^{non\text{-}V600E}$ cohorts using univariate and multivariate logistic regression analysis

The numbers and percentages of categorical variables were calculated in the *BRAF*^{V600E} and *BRAF*$^{non\text{-}V600E}$ groups. The available data for co-occurring mutated genes in these two groups were analyzed using univariate logistic regression analysis. Thereafter, significant variables ($P < 0.10$) were analyzed using multivariate logistic regression analysis. The ORs and 95% CIs were estimated.

Co-occurring copy number alterations in the *BRAF*^{V600E} and *BRAF*$^{non\text{-}V600E}$ cohorts using heatmap and univariate logistic regression analysis

The available copy number alterations of the *BRAF*^{V600E} and *BRAF*$^{non\text{-}V600E}$ cohorts were retrieved and displayed using a heatmap by Morpheus (https://software.broadinstitute.org/morpheus). The putative copy-number alterations are as follows: − 2 = homozygous deletion; − 1 = hemizygous deletion; 0 = neutral/no change; 1 = gain; 2 = high-level amplification. Univariate logistic regression analysis was used to calculate the numbers and percentages of *CDKN2A* homozygous deletion (HD) and *CDKN2B* HD. The ORs and 95% CIs were estimated.

Crossover analysis with Kaplan–Meier survival curves and the log rank (mantel-Cox) test

The overall survival rates of the *BRAF*^{V600E} and *BRAF*-$^{non\text{-}V600E}$ cohorts were compared using Kaplan-Meier curves and the log rank (Mantel-Cox) test [23]. To exclude the benefit of *IDH1/2* on survival, we referred to the *BRAF*^{V600E} & *IDH1/2*^{WT} group as the *BRAF*^{V600E} group minus those with *IDH1/2* mutations, as well the *BRAF* $^{non\text{-}V600E}$ & *IDH1/2*^{WT} group as the *BRAF* $^{non\text{-}V600E}$ group minus those with *IDH1/2* mutations. The survival of the *BRAF*^{V600E} & *IDH1/2*^{WT} group was compared with that of the *BRAF*$^{non\text{-}V600E}$ & *IDH1/2*^{WT} groups. There were two clusters of mutations, one in the glycine-rich loop (referred to as the G-loop) and the other in the activation segment. To evaluate the effect of the mutation site on survival, we defined two subgroups in the *BRAF*$^{non\text{-}V600E}$ & *IDH1/2*^{WT} group. One subgroup was the *BRAF*$^{non\text{-}V600E}$ & *IDH1/2*^{WT} group with the mutation site in the G-loop, and the other subgroup was the *BRAF*$^{non\text{-}V600E}$ & *IDH1/2*^{WT} group with the mutation site in the activation segment. The *BRAF*^{V600E} & *IDH1/2*^{WT} group was compared with those two subgroups. Furthermore, the G-loop *BRAF*$^{non\text{-}V600E}$ & *IDH1/2*^{WT} subgroup was compared with the remaining patients in the *BRAF*$^{non\text{-}V600E}$ & *IDH1/2*^{WT} group.

Statistical analysis

Major characteristics, co-occurring mutations and copy number alterations of the *BRAF*^{V600E} and *BRAF*$^{non\text{-}V600E}$ cohorts were analyzed using univariate logistic regression analysis. Significant variables ($P < 0.10$) of co-occurring mutations of the *BRAF*^{V600E} and *BRAF*$^{non\text{-}V600E}$ cohorts were analyzed using multivariate logistic regression analysis. Kaplan-Meier curves were generated for glioma patients with *BRAF* mutations and were compared using the log-rank (Mantel-Cox) test. A P value < 0.05 was considered statistically significant.

Results

Data enrollment in the study

In all 20 CNS/brain studies (6164 samples), 4674 samples with mutation data were queried; 90 samples (90 patients) with *BRAF* mutations, including 53 samples (53 patients) with *BRAF*^{V600E} and 37 samples (37 patients) with *BRAF*$^{non\text{-}V600E}$, are shown in Table 1. The cancer types of 20 CNS/brain studies included diffuse glioma, glioblastoma, oligodendroglioma, embryonal tumor, encapsulated glioma, and miscellaneous neuroepithelial tumor. The scheme for the final enrolled and investigated data is shown in Fig. 1. Ninety patients with *BRAF*^{V600E} or *BRAF*$^{non\text{-}V600E}$ were enrolled in this study, and data from 52 nonredundant patients were investigated. The integrated data of their major patient characteristics, including sex, age, diagnosis age, cancer type, data of co-occurring mutations, copy number alterations, and overall survival time and status, were collected for further analysis.

Major characteristics of the cohorts with *BRAF*^{V600E} and *BRAF*$^{non\text{-}V600E}$

The study populations were divided into two groups, *BRAF*^{V600E} and *BRAF*$^{non\text{-}V600E}$. The major demographic characteristics and clinical data of the two groups are summarized in Table 2. The patients' ages ranged from 20 to 85 years and were divided into early adulthood, midlife, mature adulthood, and late adulthood (aged 20–35, 35–50, 50–80, and > 80 years, respectively). The two groups had comparable proportions of male patients, diagnosis age, cancer type, and overall survival status. Glioblastoma multiform was the most common cancer type in both cohorts (74.07% vs. 56.00%; $P = 0.175$; Table 2).

Co-occurring mutations of the *BRAF*^{V600E} and *BRAF*$^{non\text{-}V600E}$ cohorts using univariate and multivariate logistic regression analysis

Available co-occurring gene mutations of *the BRAF*^{V600E} and *BRAF*$^{non\text{-}V600E}$ cohorts were retrieved, and differences

Table 1 The CNS/brain projects of TCGA database enrolled in the study retrieved by cBioPortal

Project	All Samples	Samples with mutation data	Samples with *BRAF*^{V600E}	Samples with *BRAF*$^{non\text{-}V600E}$	References
Diffuse Glioma					
Brain Lower Grade Glioma (TCGA, Firehose Legacy)	530	286	1	1	https://www.cancer.gov
Brain Lower Grade Glioma (TCGA, PanCancer Atlas)	514	512	1	2	[24–29]
Glioma (MSK, Nature 2019)	91	91	2	1	https://www.cancer.gov
Glioma (MSKCC, Clin Cancer Res 2019)	1004	1004	22	19	[30]
Low-Grade Gliomas (UCSF, Science 2014)	61	61	2	0	[31]
Merged Cohort of LGG and GBM (TCGA, Cell 2016)	1102	812	5	2	[32]
GLIOBLASTOMA					
Brain Tumor PDXs (Mayo Clinic, 2019)	95	83	2	1	https://www.cbioportal.org
Glioblastoma (Columbia, Nat Med. 2019)	42	32	1	1	[33]
Glioblastoma (TCGA, Cell 2013)	543	257	3	0	[34]
Glioblastoma (TCGA, Nature 2008)	206	91	0	0	[35]
Glioblastoma Multiforme (TCGA, Firehose Legacy)	604	290	5	1	https://www.cancer.gov
Glioblastoma Multiforme (TCGA, PanCancer Atlas)	592	397	5	3	[24–29, 36]
OLIGODENDROGLIOMA					
Anaplastic Oligodendroglioma and Anaplastic Oligogastrocytoma (MSKCC, Neuro Oncol 2017)	22	22	0	0	[37]
Embryonal Tumor					
MEDULLOBLASTOMA					
Medulloblastoma (Broad, Nature 2012)	92	92	0	0	[38]
Medulloblastoma (ICGC, Nature 2012)	125	125	0	0	[39]
Medulloblastoma (PCGP, Nature 2012)	37	37	0	0	[40]
Medulloblastoma (Sickkids, Nature 2016)	46	46	0	1	[41]
Encaspulated Glioma					
PILOCYTIC ASTROCYTOMA					
Pilocytic Astrocytoma (ICGC, Nature Genetics 2013)	96	96	4	3	[42]
Miscellaneous Neuroepithelial Tumor					
Pheochromocytoma and Paraganglioma (TCGA, Cell 2017)	178	178	0	1	[43]
Pheochromocytoma and Paraganglioma (TCGA, Firehose Legacy)	184	162	0	1	https://www.cancer.gov

between the two groups were compared; the results are summarized in Table 3. The mutation frequencies of *KRAS*, *HRAS*, *RAF1*, *MAP 3 K1*, *MAP 2 K1*, *MAP 2 K2*, *MAP 2 K4*, *MDM2*, *MDM4*, *CDKN2A*, and *CDKN2B* were comparable between the two groups. In contrast, the *BRAF*$^{non\text{-}V600E}$ group exhibited a significantly higher mutation frequency of *TP53* (56.00% vs. 7.41%; $P = 0.001$), *IDH1/2* (36.00% vs. 3.70%; $P = 0.015$), and *ATRX* (32.00% vs. 7.41%; $P = 0.037$) than the *BRAF*^{V600E} group. The variables with $P < 0.10$ were analyzed using multivariate logistic regression analysis, and the *BRAF*$^{non\text{-}V600E}$ group exhibited a significantly higher *TP53* mutation frequency (56.00% vs. 7.41%; $P = 0.031$) than the *BRAF*^{V600E} group (Table 3).

Co-occurring copy number alteration in the *BRAF*^{V600E} and *BRAF*$^{non\text{-}V600E}$ cohorts using heatmap and univariate logistic regression analysis

There were no available copy number data for five patients with *BRAF*^{V600E} and five patients with *BRAF*$^{non\text{-}V600E}$. The copy number alterations of the available co-occurring genes included *BRAF*, *RAF1*, *MAP 3 K1*, *MAP 2 K1*, *MAP 2 K2*, *MAP 2 K4*, *MAPK1*, *MAPK3*, *TP53*, *MDM2*, *MDM4*, *TP53BP1*, *IDH1*, *IDH2*, *ATRX*, *CDKN2A*, and *CDKN2B*. The HD copy number was frequently retrieved for these two genes, including *CDKN2A* and *CDKN2B* (Fig. 2), and the HD of both *CDKN2A* (77.27.00% vs. 60.00%; $P = 0.032$) and *CDKN2B* (77.27.00% vs. 60.00%; $P = 0.032$) was more frequent in

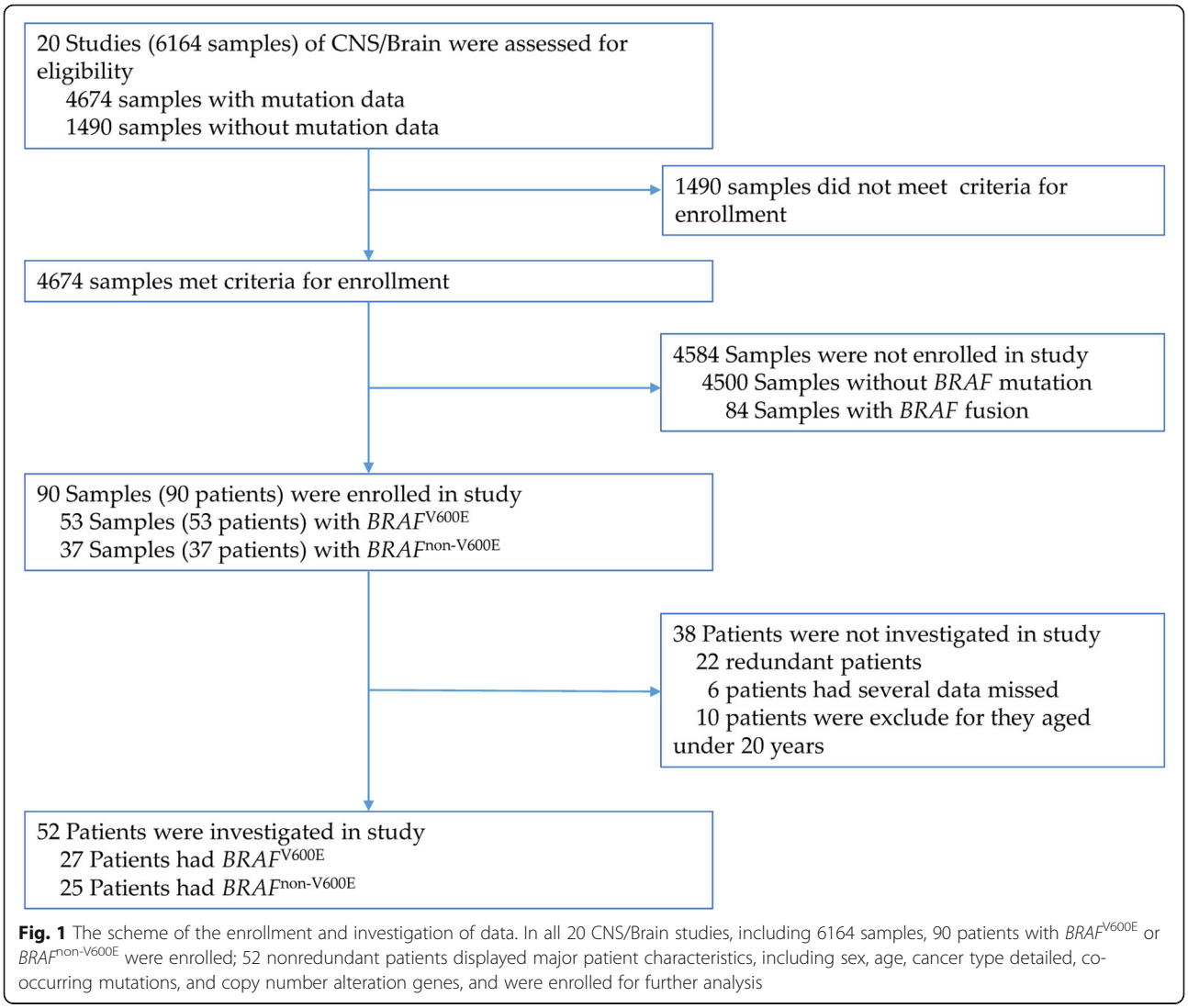

Fig. 1 The scheme of the enrollment and investigation of data. In all 20 CNS/Brain studies, including 6164 samples, 90 patients with *BRAF*^{V600E} or *BRAF*$^{non\text{-}V600E}$ were enrolled; 52 nonredundant patients displayed major patient characteristics, including sex, age, cancer type detailed, co-occurring mutations, and copy number alteration genes, and were enrolled for further analysis

the *BRAF*^{V600E} cohort than in the *BRAF*$^{non\text{-}V600E}$ cohort (Table 4).

Crossover analysis using Kaplan–Meier survival curves and the log-rank (mantel-Cox) test

Crossover Kaplan–Meier survival curves and the log-rank (Mantel-Cox) test were performed to explore the difference between the overall survival of glioma patients with *BRAF*^{V600E} and *BRAF*$^{non\text{-}V600E}$. The estimated mean survival time was 51.394 months for patients with *BRAF*^{V600E}, 89.958 months for patients with *BRAF*-$^{non\text{-}V600E}$, 44.500 months for patients with *BRAF*^{V600E} & *IDH1/2*^{WT}, and 93.821 months for patients with *BRAF*-$^{non\text{-}V600E}$ & *IDH1/2*^{WT}. There was no difference between the survival of *BRAF*^{V600E} and *BRAF*$^{non\text{-}V600E}$ (51.394 vs. 89.958, chi-square 1.130, $P = 0.288$). In addition, there was no difference between the survival of *BRAF*^{V600E} & *IDH1/2*^{WT} and *BRAF*$^{non\text{-}V600E}$ & *IDH1/2*^{WT} (44.500 vs. 93.821, chi-square 0.007, $P = 0.935$), which excluded the survival benefit of *IDH1/2*. We also evaluated the survival of *BRAF*$^{non\text{-}V600E}$ & *IDH1/2*^{WT} with mutations in the G-loop and activation segment. The estimated survival time of these two subgroups was 12.250 months for patients with *BRAF*$^{non\text{-}V600E}$ & *IDH1/2*^{WT} with mutations in the G-loop and 34.800 months for patients with *BRAF*$^{non\text{-}V600E}$ & *IDH1/2*^{WT} with mutations in the activation segment. In addition, there was no difference between the *BRAF*^{V600E} & *IDH1/2*^{WT} cohorts and those of the *BRAF*$^{non\text{-}V600E}$ & *IDH1/2*^{WT} cohorts. As shown below, *BRAF*^{V600E} & *IDH1/2*^{WT} vs. *BRAF*$^{non\text{-}V600E}$ & *IDH1/2*^{WT} had mutations in the G-loop (44.500 vs. 12.250, chi-squared 0.122, $P = 0.727$), and *BRAF*^{V600E} & *IDH1/2*^{WT} vs. *BRAF*$^{non\text{-}V600E}$ & *IDH1/2*^{WT} had mutations in the activation segment (44.500 vs. 34.800, chi-square 0.145, $P = 0.703$). Since the estimated mean survival of *BRAF*$^{non\text{-}V600E}$ & *IDH1/2*^{WT} with mutations

Table 2 The major characteristics of cohorts including $BRAF^{V600E}$ and $BRAF^{non\text{-}V600E}$

Variables	$BRAF^{V600E}$ ($n = 27$)		$BRAF^{non\text{-}V600E}$ ($n = 25$)		Univariate analysis		
	Number	%	Number	%	Odds Ratio	95% Confidence Interval	*P* Value
Male	16	59.26	18	72.00	0.566	0.177–1.809	0.337
Diagnosis Age							
Ages 20–35	9	33.33	6	24.00	1.583	0.469–5.350	0.459
Ages 36–50	9	33.33	8	32.00	1.062	0.333–3.390	0.918
Ages 51–80	7	25.93	11	44.00	0.445	0.139–1.433	0.175
Age 80+	2	7.41	0	0.00	1,615,474,843	0.000-	0.999
Cancer type detailed							
Glioblastoma Multiform	20	74.07	14	56.00	2.245	0.698–7.219	0.175
Astrocytoma	3	11.11	6	24.00	0.396	0.087–1.794	0.229
Oligoastrocytoma	1	3.70	0	0.00	1,553,341,195	0.000-	1.000
Oligodendroglioma	0	0.00	3	12.00	0.000	0.000-	0.999
Gliosarcoma	0	0.00	2	8.00	0.000	0.000-	0.999
Other glioma	3	11.11	0	0.00	1,682,786,295	0.000-	0.999
Overall survival status							
Deceased	14	51.85	11	44.00	1.371	0.460–4.087	0.572

in the G-loop was the shortest, we compared the $BRAF^{non\text{-}V600E}$ & $IDH1/2^{WT}$ with mutations in the G-loop with the remaining $BRAF^{non\text{-}V600E}$ & $IDH1/2^{WT}$ patients. There was no difference between them (12.250 vs. 95.100, chi-square 0.008, $P = 0.927$) (Fig. 3). The numbers at risk of Kaplan–Meier survival curves were shown in Supplementary Dataset S2.

Discussion

BRAF mutations critically affect cancer growth and progression and are supposed to be a founder event for mutations occurring early in the initiation process of cancer. However, *BRAF* mutations must cooperate with other mechanisms for a fully cancerous state, as they are insufficient to induce cancer alone [5]. $BRAF^{V600E}$ has

Table 3 The co-occurred mutations of $BRAF^{V600E}$ and $BRAF^{non\text{-}V600E}$ cohort using univariate and multivariate logistics regression analysis

Gene	$BRAF^{V600E}$ ($n = 27$)		$BRAF^{non\text{-}V600E}$ ($n = 25$)		Univariate analysis			Multivariate analysis		
	Number	%	Number	%	Odds Ratio	95% Confidence Interval	*P* Value	Odds Ratio	95% Confidence Interval	*P* Value
KRAS	0	0.00	1	4.00	1,817,409,198	0.000-	1.000			
HRAS	0	0.00	1	4.00	1,817,409,198	0.000-	1.000			
RAF1	0	0.00	2	8.00	1,896,426,989	0.000-	0.999			
MAP 3 K1	1	3.70	6	24.00	8.211	0.911–73.959	0.060			
MAP 2 K1	0	0.00	2	8.00	1,896,426,989	0.000-	0.999			
MAP 2 K2	0	0.00	4	16.00	2,077,039,084	0.000-	0.999			
MAP 2 K4	0	0.00	2	8.00	1,896,426,989	0.000-	0.999			
TP53	2	7.41	14	56.00	15.909	3.078–82.224	0.001	12.186	1.251–118.721	0.031
MDM2	1	3.70	3	12.00	3.545	0.344–36.561	0.298			
MDM4	0	0.00	4	16.00	2,077,039,084	0.000-	0.999			
CDKN2A	0	0.00	3	12.00	1,982,628,216	0.000-	0.999			
CDKN2B	0	0.00	1	4.00	1,817,409,198	0.000-	1.000			
IDH1/2	1	3.70	9	36.00	14.625	1.690–126.537	0.015	5.498	0.512–59.020	0.159
ATRX	2	7.41	8	32.00	5.882	1.110–31.170	0.037	0.665	0.048–9.188	0.761

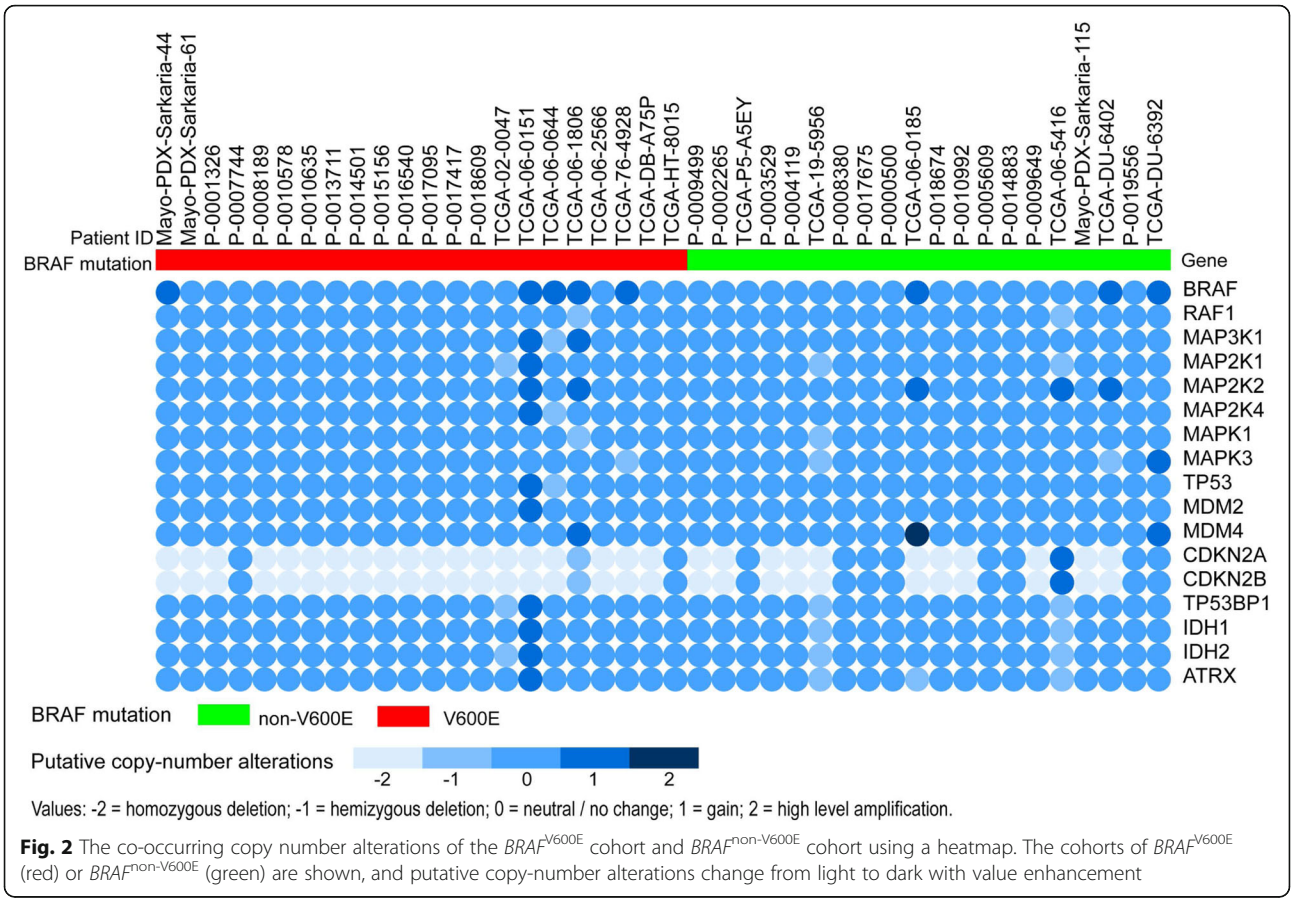

Fig. 2 The co-occurring copy number alterations of the *BRAF*^{V600E} cohort and *BRAF*$^{non\text{-}V600E}$ cohort using a heatmap. The cohorts of *BRAF*^{V600E} (red) or *BRAF*$^{non\text{-}V600E}$ (green) are shown, and putative copy-number alterations change from light to dark with value enhancement

been the mutation of interest in previous studies on glioma, especially in pediatric glioma patients, for the available molecule-targeted drugs. However, various *BRAF*$^{non\text{-}V600E}$ cells exert different activation effects on the MAPK pathway. The exact impact on the clinical prognosis and possible molecular mechanism of associated co-occurring genes with mutations or copy number alterations co-occurring with *BRAF* mutations remains unclear in adult glioma patients. In this study, the available data of patients with *BRAF*$^{non\text{-}V600E}$ and *BRAF*^{V600E} in the TCGA CNS/brain database were investigated to determine the possible mechanisms of *BRAF* gene mutations in adult glioma patients.

Our data indicated that in adult glioma patients with *BRAF* mutations, including both *BRAF*$^{non\text{-}V600E}$ and *BRAF*^{V600E} cohorts, glioblastoma multiform was the most common cancer type. A previous study showed that all *BRAF*^{V600E} glioblastomas were primary tumors in both pediatric and adult patients [44]. Tabouret et al. [20] reported a case the co-occurrence of both *IDH1* mutation and *BRAF*^{V600E} although those two mutations are mutually exclusive in glial tumor. The available co-occurring mutated genes in the MAPK and p53 pathways showed that mutated genes frequently co-occurred in the *BRAF*$^{non\text{-}V600E}$ cohort, and there were more *TP53*, *IDH1/2*, and *ATRX* mutations in *BRAF*$^{non\text{-}V600E}$ than in *BRAF*^{V600E}. Lai et al. [45] found that a *TP53* point mutation at position 273 (Arg to Cys) was more common than *IDH1* mutations at position 132 (Arg to His). They hypothesized that the *TP53* mutation (C → T) occurred in the nontranscribed strand, while the *IDH1* mutation existed in the transcribed strand, which is a strand asymmetry pattern [46]. Another study indicated that *IDH1/2* mutations represent early events in brain tumor

Table 4 *CDKN2A/2B* HD of *BRAF*^{V600E} and *BRAF*$^{non\text{-}V600E}$ cohort using univariate logistics regression analysis

Variables	*BRAF*^{V600E} (*n* = 22)		*BRAF*$^{non\text{-}V600E}$ (*n* = 20)		Univariate analysis		
	Number	%	Number	%	Odds Ratio	95% Confidence Interval	*P* Value
CDKN2A	17	77.27	12	60.00	0.193	0.043–0.867	0.032
CDKN2B	17	77.27	12	60.00	0.193	0.043–0.867	0.032

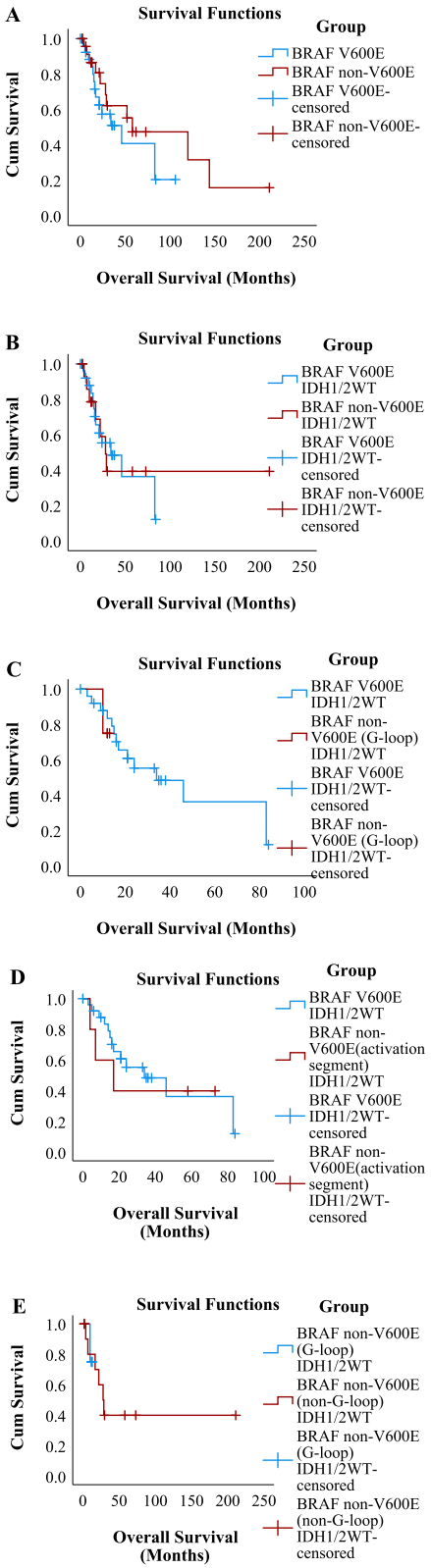

Fig. 3 Crossover analysis with Kaplan–Meier survival curves and the log-rank (Mantel-Cox) test. **a** $BRAF^{V600E}$ vs. $BRAF^{non\text{-}V600E}$ (51.394 vs. 89.958, Chi-Square 1.130, $P = 0.288$); **b** $BRAF^{V600E}$ & $IDH1/2^{WT}$ vs. $BRAF^{non\text{-}V600E}$ & $IDH1/2^{WT}$ (44.500 vs. 93.821, Chi-Square 0.007, $P = 0.935$); **c** $BRAF^{V600E}$ & $IDH1/2^{WT}$ vs. $BRAF^{non\text{-}V600E}$ & $IDH1/2^{WT}$ with mutations in G-loop (44.500 vs. 12.250, Chi-Square 0.122, $P = 0.727$); **d** $BRAF^{V600E}$ & $IDH1/2^{WT}$ vs. $BRAF^{non\text{-}V600E}$ & $IDH1/2^{WT}$ with mutations in activation segment (44.500 vs. 34.800, Chi-Square 0.145, $P = 0.703$); **e** $BRAF^{non\text{-}V600E}$ & $IDH1/2^{WT}$ with mutations in G-loop vs. the rest $BRAF^{non\text{-}V600E}$ & $IDH1/2^{WT}$ patients (12.250 vs. 95.100, Chi-Square 0.008, $P = 0.927$)

formation [47]. Liu et al. [48] found that *ATRX* alterations correlated with mutations in *IDH1/2* and *TP53* in glioma of all grades. It has been reported that *ATRX* deletions/mutations are correlated with *TP53* and *IDH1* mutations [49, 50]. Somatic *TP53*, *ATRX*, and *IDH1/2* mutations have been found in adult LGGs [51]. *ATRX* mutations are detected in adult diffuse gliomas and astrocytomas harboring both *TP53* and *IDH1/2*. The co-occurrence of these three mutated genes, including *TP53*, *IDH1/2*, and *ATRX*, facilitates the growth of an adult diffuse astrocytoma subgroup [48]. All of the studies above indicate that *ATRX* mutations frequently overlap with *IDH1/2* and *TP53* mutations. In the present study, we also found the co-occurrence of these three mutations, which were frequently detected in the $BRAF^{non\text{-}V600E}$ cohort but not in the $BRAF^{V600E}$ cohort. Our findings indicated that in adult glioma patients, a possible correlation between $BRAF^{non\text{-}V600E}$ and these three common mutations simultaneously occurred in glioma. Multivariate logistic regression revealed that *TP53* was an independent risk factor in the $BRAF^{non\text{-}V600E}$ cohort vs. the $BRAF^{V600E}$ group. Our data demonstrated a correlation between $BRAF^{non\text{-}V600E}$ and *TP53* mutations in adult glioma patients.

Previous findings have shown that active *Ras* can induce heterodimerization of *BRAF* and *RAF1* [52] and that this event may be critical for *RAF1* activation [53]. *RAF1* directly regulates cell apoptosis, which does not depend on MAPK signaling [54, 55], but occurs through direct interaction with *Bcl-2* [54]. *TP53* can regulate *Bcl-2* by suppressing *Bcl-2* transcription [56]. We proposed that the $BRAF^{non\text{-}V600E}$ mutation might activate the *BRAF-RAF1* heterodimer, which shows antiapoptotic properties via the activation of Bcl-2 through *RAF1* phosphorylation. Mutant *TP53*, which is frequently accompanied by *IDH1/2* mutation by a strand asymmetry mechanism, fails to regulate *Bcl-2*. Therefore, with both activated *RAF1* and mutated *TP53*, an enhanced antiapoptotic effect, which promotes cancer growth, might be predicted.

Compared to BRAF fusions, $BRAF^{V600E}$ tends to be more aggressive, more likely to be associated with *CDKN2A/B* deletions, and can transform cancers into higher-grade tumors [57, 58]. Our data showed that

CDKN2A and *CDKN2B* HDs were more frequent in the $BRAF^{V600E}$ cohort than in the $BRAF^{non\text{-}V600E}$ cohort. Concomitant *CDKN2A* and *CDKN2B* HDs could be detected in patients with glioblastoma multiform cancer, astrocytoma, and gliosarcoma. A previous report indicated that five of seven pediatric grade II–IV astrocytomas with $BRAF^{V600E}$ had concomitant *CDKN2A* HD [59] and *CDKN2A* deletions combined with $BRAF^{V600E}$ alterations, constituting a subgroup of secondary high-grade gliomas [60]. We found that in adult glioma patients, $BRAF^{V600E}$ and $BRAF^{non\text{-}V600E}$ frequently co-occurred with *CDKN2A* HDs combined with *CDKN2B* HDs, especially in patients with $BRAF^{V600E}$. Except for astrocytoma, glioblastoma multiform cancer was the most common cancer type with these combined alterations. Robinson et al. [61] indicated that activated Akt or Ink4a/ARF deletions are necessary for high-grade brain neoplasms with *BRAF* mutations in a Cre/lox animal model. Our results showed the possible synergy of *CDKN2A* and *CDKN2B* HDs with *BRAF* mutations, especially in adult glioma patients with $BRAF^{V600E}$ and $BRAF^{non\text{-}V600E}$.

$BRAF^{V600E}$ reportedly enhances *BRAF* kinase activity 500-fold [62]. According to its kinase viability, $BRAF^{non\text{-}V600E}$ mutations can be classified into three groups: high activity (130–700 times), intermediate activity (1.3–64 times), and impaired activity (30–80%) [16]. Theoretically, the higher the *BRAF* kinase activity, the worse the prognosis. To clarify whether there is a difference between $BRAF^{V600E}$ and $BRAF^{non\text{-}V600E}$, we compared the overall survival of these two cohorts, and no statistical significance was found.

In addition, the status of *IDH* mutations in glioblastomas definitely influences the prognosis of patients with glioblastomas; therefore, *IDH*-wildtype glioblastomas are defined as primary tumors, while *IDH*-mutant glioblastomas are classified as secondary tumors [63]. To exclude the benefit of *IDH* mutations on survival, we compared the $BRAF^{V600E}$ & $IDH1/2^{WT}$ and $BRAF^{non\text{-}V600E}$ & $IDH1/2^{WT}$ cohorts, and no difference was detected. The positions of the G-loop and the activation segment are 458–470 aa and 577–622 aa in BRAF, respectively [64]. Most $BRAF^{non\text{-}V600E}$ mutations exist in the G-loop and the activation segment [16, 64]; therefore, we selected the two cohorts as $BRAF^{non\text{-}V600E}$ & $IDH1/2^{WT}$ with mutations in the G-loop and activation segment. We compared them with $BRAF^{V600E}$ & $IDH1/2^{WT}$, and no difference was found between the $BRAF^{V600E}$ & $IDH1/2^{WT}$ cohorts and those of the $BRAF^{non\text{-}V600E}$ & $IDH1/2^{WT}$ cohorts. Furthermore, we compared $BRAF^{non\text{-}V600E}$ & $IDH1/2^{WT}$ with mutations in the G-loop with the remaining $BRAF^{non\text{-}V600E}$ & $IDH1/2^{WT}$ patients and found no difference between them. Although there was no statistical significance, the estimated mean survival of $BRAF^{non\text{-}V600E}$ & $IDH1/2^{WT}$ with mutations in the G-loop was the shortest in all cohorts. We propose that a larger sample is necessary for confirmation of this finding. Our data indicated that the $BRAF^{non\text{-}V600E}$ cohort had no survival advantage from co-occurrence with *IDH* mutations compared with the $BRAF^{non\text{-}V600E}$ cohort of adult patients with glioma.

Limitations

Because the $BRAF^{V600E}$ mutation is rare in adult glioma, there were few patients in both cohorts retrieved from the publicly available data (cBioPortal). In this study, while their apparent survival times were substantially different, they were not significantly different. To prove the mechanism by which *BRAF* mutations promote cancer growth via an enhanced antiapoptotic effect of *Bcl-2*, further study using appropriate clinical tissue samples or animal models are necessary.

Conclusions

In conclusion, we found that in adult patients with gliomas, $BRAF^{non\text{-}V600E}$, rather than $BRAF^{V600E}$, frequently co-occurs with *TP53*, *IDH1/2*, and *ATRX* mutations. Both $BRAF^{non\text{-}V600E}$ and $BRAF^{V600E}$ frequently overlapped with *CDKN2A/2B* HDs, whereas there were no significant differences between the two cohorts. Although there were significant differences in co-occurring gene mutations and copy number alterations, no difference was found in survival between cohorts of $BRAF^{non\text{-}V600E}$ and $BRAF^{V600E}$ with and without IDH1/2 favorable effects on survival. We also found that the estimated mean survival of $BRAF^{non\text{-}V600E}$ & $IDH1/2^{WT}$ with mutations in the G-loop was the shortest; however, no difference was observed between that cohort and other cohorts. Due to the poor available mRNA and protein data in the TCGA database we retrieved in this study, no expression data were evaluated. More clinical data or models are necessary to elucidate the mechanism involved in $BRAF^{non\text{-}V600E}$-associated glioma in the future.

Abbreviations

HD: Homozygous deletion; *BRAF*: v-raf murine sarcoma viral oncogene homolog B1; LGGs: Low-grade gliomas; TCGA: The Cancer Genome Atlas; ORs: Odds ratios; Cis: Confidence intervals; G-loop: Glycine-rich loop; MAPK: Mitogen-activated protein kinase

Supplementary Information

The online version contains supplementary material available at https://doi.org/10.1186/s12883-021-02224-6.

Additional file 1.

Additional file 2.

Acknowledgements

The results published or shown here are in whole or part based upon public data generated by the TCGA Research Network: https://www.cancer.gov/tcga.

Authors' contributions
WW: Formal analysis, Writing- Original draft preparation. MW: Writing-Reviewing & Editing. HJ: Investigation. TW: Data curation. RD: Conceptualization, Methodology. All authors read and approved the final manuscript.

Funding
This study was financially supported by the Natural Science Basic Research Program of Shaanxi (Program No. 2018JM7062), and The Project of The First Affiliated Hospital of Xi'an Jiaotong University (XJYFY-2019w33).

Availability of data and materials
All data generated or analyzed during this study are included in this published article and its supplementary information files.

Declarations

Ethics approval and consent to participate
Not applicable.

Consent for publication
Not applicable.

Competing interests
The authors declare that they have no competing interests.

Author details
[1]Department of Neurosurgery, The First Affiliated Hospital of Xi'an Jiaotong University, Xi'an, China. [2]Department of Clinical Laboratory, The First Affiliated Hospital of Xi'an Jiaotong University, No.277 Yanta West Road, Xi'an 710061, Shaanxi, China.

Received: 6 March 2021 Accepted: 5 May 2021
Published online: 12 May 2021

References
1. Mercer KE, Pritchard CA. Raf proteins and cancer: B-Raf is identified as a mutational target. Biochim Biophys Acta. 2003;1653(1):25–40. https://doi.org/10.1016/s0304-419x(03)00016-7.
2. Roskoski R Jr. RAF protein-serine/threonine kinases: structure and regulation. Biochem Biophys Res Commun. 2010;399(3):313–7. https://doi.org/10.1016/j.bbrc.2010.07.092.
3. Basto D, Trovisco V, Lopes JM, Martins A, Pardal F, Soares P, et al. Mutation analysis of B-RAF gene in human gliomas. Acta Neuropathol. 2005;109(2):207–10. https://doi.org/10.1007/s00401-004-0936-x.
4. Kaltsas P, Want S, Cohen J. Development of a time-to-positivity assay as a tool in the antibiotic management of septic patients. Clin Microbiol Infect. 2005;11(2):109–14. https://doi.org/10.1111/j.1469-0691.2004.01054.x.
5. Dhomen N, Marais R. New insight into BRAF mutations in cancer. Curr Opin Genet Dev. 2007;17(1):31–9. https://doi.org/10.1016/j.gde.2006.12.005.
6. Network TCGAR. Comprehensive molecular profiling of lung adenocarcinoma. Nature. 2014;511(7511):543–50.
7. Davies H, Bignell GR, Cox C, Stephens P, Edkins S, Clegg S, et al. Mutations of the BRAF gene in human cancer. Nature. 2002;417(6892):949–54. https://doi.org/10.1038/nature00766.
8. Barnier JV, Papin C, Eychene A, Lecoq O, Calothy G. The mouse B-raf gene encodes multiple protein isoforms with tissue-specific expression. J Biol Chem. 1995;270(40):23381–9. https://doi.org/10.1074/jbc.270.40.23381.
9. Catling AD, Reuter CW, Cox ME, Parsons SJ, Weber MJ. Partial purification of a mitogen-activated protein kinase kinase activator from bovine brain. Identification as B-Raf or a B-Raf-associated activity. J Biol Chem. 1994;269(47):30014–21. https://doi.org/10.1016/S0021-9258(18)43982-8.
10. Xie P, Streu C, Qin J, Bregman H, Pagano N, Meggers E, et al. The crystal structure of BRAF in complex with an organoruthenium inhibitor reveals a mechanism for inhibition of an active form of BRAF kinase. Biochemistry. 2009;48(23):5187–98. https://doi.org/10.1021/bi802067u.
11. Raabe EH, Lim KS, Kim JM, Meeker A, Mao XG, Nikkhah G, et al. BRAF activation induces transformation and then senescence in human neural stem cells: a pilocytic astrocytoma model. Clin Cancer Res. 2011;17(11):3590–9. https://doi.org/10.1158/1078-0432.CCR-10-3349.
12. Schindler G, Capper D, Meyer J, Janzarik W, Omran H, Herold-Mende C, et al. Analysis of BRAF V600E mutation in 1,320 nervous system tumors reveals high mutation frequencies in pleomorphic xanthoastrocytoma, ganglioglioma and extra-cerebellar pilocytic astrocytoma. Acta Neuropathol. 2011;121(3):397–405. https://doi.org/10.1007/s00401-011-0802-6.
13. Behling F, Barrantes-Freer A, Skardelly M, Nieser M, Christians A, Stockhammer F, et al. Frequency of BRAF V600E mutations in 969 central nervous system neoplasms. Diagn Pathol. 2016;11(1):55. https://doi.org/10.1186/s13000-016-0506-2.
14. Behling F, Schittenhelm J. Oncogenic BRAF alterations and their role in brain tumors. Cancers (Basel). 2019;11(6):794.
15. Woods D, Parry D, Cherwinski H, Bosch E, Lees E, McMahon M. Raf-induced proliferation or cell cycle arrest is determined by the level of Raf activity with arrest mediated by p21Cip1. Mol Cell Biol. 1997;17(9):5598–611. https://doi.org/10.1128/MCB.17.9.5598.
16. Wan PT, Garnett MJ, Roe SM, Lee S, Niculescu-Duvaz D, Good VM, et al. Mechanism of activation of the RAF-ERK signaling pathway by oncogenic mutations of B-RAF. Cell. 2004;116(6):855–67. https://doi.org/10.1016/S0092-8674(04)00215-6.
17. Komori T. The 2016 WHO classification of Tumours of the central nervous system: the major points of revision. Neurol Med Chir (Tokyo). 2017;57(7):301–11. https://doi.org/10.2176/nmc.ra.2017-0010.
18. Parsons DW, Jones S, Zhang X, Lin JC, Leary RJ, Angenendt P, et al. An integrated genomic analysis of human glioblastoma multiforme. Science. 2008;321(5897):1807–12. https://doi.org/10.1126/science.1164382.
19. Zhang C, Moore LM, Li X, Yung WK, Zhang W. IDH1/2 mutations target a key hallmark of cancer by deregulating cellular metabolism in glioma. Neuro-Oncology. 2013;15(9):1114–26. https://doi.org/10.1093/neuonc/not087.
20. Tabouret E, Fina F, Vincentelli F, Nanni I, Figarella-Branger D. New IDH1 I113T mutation associated with BRAF V600E mutation: new driver of gliomagenesis? J Neurol Sci. 2014;342(1–2):204–6. https://doi.org/10.1016/j.jns.2014.05.010.
21. Cerami E, Gao J, Dogrusoz U, Gross BE, Sumer SO, Aksoy BA, et al. The cBio cancer genomics portal: an open platform for exploring multidimensional cancer genomics data. Cancer Discov. 2012;2(5):401–4. https://doi.org/10.1158/2159-8290.CD-12-0095.
22. Gao J, Aksoy BA, Dogrusoz U, Dresdner G, Gross B, Sumer SO, et al. Integrative analysis of complex cancer genomics and clinical profiles using the cBioPortal. Sci Signal. 2013;6(269):pl1. https://doi.org/10.1126/scisignal.2004088.
23. Kleinbaum DG, Klein M. Kaplan–Meier Survival Curves and the Log–Rank Test; 1996.
24. Hoadley KA, Yau C, Hinoue T, Wolf DM, Lazar AJ, Drill E, et al. Cell-of-origin patterns dominate the molecular classification of 10,000 tumors from 33 types of Cancer. Cell. 2018;173(2):291–304 e6. https://doi.org/10.1016/j.cell.2018.03.022.
25. Ellrott K, Bailey MH, Saksena G, Covington KR, Kandoth C, Stewart C, et al. Scalable Open Science approach for mutation calling of tumor exomes using multiple genomic pipelines. Cell Syst. 2018;6(3):271–81 e7. https://doi.org/10.1016/j.cels.2018.03.002.
26. Taylor AM, Shih J, Ha G, Gao GF, Zhang X, Berger AC, et al. Genomic and functional approaches to understanding Cancer aneuploidy. Cancer Cell. 2018;33(4):676–89 e3. https://doi.org/10.1016/j.ccell.2018.03.007.
27. Gao Q, Liang WW, Foltz SM, Mutharasu G, Jayasinghe RG, Cao S, et al. Driver fusions and their implications in the development and treatment of human cancers. Cell Rep. 2018;23(1):227–38 e3. https://doi.org/10.1016/j.celrep.2018.03.050.
28. Liu J, Lichtenberg T, Hoadley KA, Poisson LM, Lazar AJ, Cherniack AD, et al. An integrated TCGA pan-Cancer clinical data resource to drive high-quality survival outcome analytics. Cell. 2018;173(2):400–16 e11.
29. Sanchez-Vega F, Mina M, Armenia J, Chatila WK, Luna A, La KC, et al. Oncogenic signaling pathways in the Cancer genome atlas. Cell. 2018;173(2):321–37 e10. https://doi.org/10.1016/j.cell.2018.03.035.
30. Jonsson P, Lin AL, Young RJ, DiStefano NM, Hyman DM, Li BT, et al. Genomic correlates of disease progression and treatment response in prospectively characterized gliomas. Clin Cancer Res. 2019;25(18):5537–47. https://doi.org/10.1158/1078-0432.CCR-19-0032.
31. Johnson BE, Mazor T, Hong C, Barnes M, Aihara K, McLean CY, et al. Mutational analysis reveals the origin and therapy-driven evolution of recurrent glioma. Science. 2014;343(6167):189–93. https://doi.org/10.1126/science.1239947.

32. Ceccarelli M, Barthel FP, Malta TM, Sabedot TS, Salama SR, Murray BA, et al. Molecular profiling reveals biologically discrete subsets and pathways of progression in diffuse glioma. Cell. 2016;164(3):550–63. https://doi.org/10.1016/j.cell.2015.12.028.
33. Zhao J, Chen AX, Gartrell RD, Silverman AM, Aparicio L, Chu T, et al. Immune and genomic correlates of response to anti-PD-1 immunotherapy in glioblastoma. Nat Med. 2019;25(3):462–9. https://doi.org/10.1038/s41591-019-0349-y.
34. Brennan CW, Verhaak RG, McKenna A, Campos B, Noushmehr H, Salama SR, et al. The somatic genomic landscape of glioblastoma. Cell. 2013;155(2):462–77. https://doi.org/10.1016/j.cell.2013.09.034.
35. Cancer Genome Atlas Research N. Comprehensive genomic characterization defines human glioblastoma genes and core pathways. Nature. 2008;455(7216):1061–8. https://doi.org/10.1038/nature07385.
36. Bhandari V, Hoey C, Liu LY, Lalonde E, Ray J, Livingstone J, et al. Molecular landmarks of tumor hypoxia across cancer types. Nat Genet. 2019;51(2):308–18. https://doi.org/10.1038/s41588-018-0318-2.
37. Thomas AA, Abrey LE, Terziev R, Raizer J, Martinez NL, Forsyth P, et al. Multicenter phase II study of temozolomide and myeloablative chemotherapy with autologous stem cell transplant for newly diagnosed anaplastic oligodendroglioma. Neuro-Oncology. 2017;19(10):1380–90. https://doi.org/10.1093/neuonc/nox086.
38. Pugh TJ, Weeraratne SD, Archer TC, Pomeranz Krummel DA, Auclair D, Bochicchio J, et al. Medulloblastoma exome sequencing uncovers subtype-specific somatic mutations. Nature. 2012;488(7409):106–10.
39. Jones DT, Jager N, Kool M, Zichner T, Hutter B, Sultan M, et al. Dissecting the genomic complexity underlying medulloblastoma. Nature. 2012;488(7409):100–5. https://doi.org/10.1038/nature11284.
40. Robinson G, Parker M, Kranenburg TA, Lu C, Chen X, Ding L, et al. Novel mutations target distinct subgroups of medulloblastoma. Nature. 2012;488(7409):43–8. https://doi.org/10.1038/nature11213.
41. Morrissy AS, Garzia L, Shih DJ, Zuyderduyn S, Huang X, Skowron P, et al. Divergent clonal selection dominates medulloblastoma at recurrence. Nature. 2016;529(7586):351–7.
42. Jones DT, Hutter B, Jager N, Korshunov A, Kool M, Warnatz HJ, et al. Recurrent somatic alterations of FGFR1 and NTRK2 in pilocytic astrocytoma. Nat Genet. 2013;45(8):927–32. https://doi.org/10.1038/ng.2682.
43. Fishbein L, Leshchiner I, Walter V, Danilova L, Robertson AG, Johnson AR, et al. Comprehensive molecular characterization of Pheochromocytoma and Paraganglioma. Cancer Cell. 2017;31(2):181–93. https://doi.org/10.1016/j.ccell.2017.01.001.
44. Dahiya S, Emnett RJ, Haydon DH, Leonard JR, Phillips JJ, Perry A, et al. BRAF-V600E mutation in pediatric and adult glioblastoma. Neuro-Oncology. 2014;16(2):318–9. https://doi.org/10.1093/neuonc/not146.
45. Rodin SN, Rodin AS. Strand asymmetry of CpG transitions as indicator of G1 phase-dependent origin of multiple tumorigenic p53 mutations in stem cells. Proc Natl Acad Sci U S A. 1998;95(20):11927–32. https://doi.org/10.1073/pnas.95.20.11927.
46. Lai A, Kharbanda S, Pope WB, Tran A, Solis OE, Peale F, et al. Evidence for sequenced molecular evolution of IDH1 mutant glioblastoma from a distinct cell of origin. J Clin Oncol. 2011;29(34):4482–90. https://doi.org/10.1200/JCO.2010.33.8715.
47. Dunn GP, Andronesi OC, Cahill DP. From genomics to the clinic: biological and translational insights of mutant IDH1/2 in glioma. Neurosurg Focus. 2013;34(2):E2. https://doi.org/10.3171/2012.12.FOCUS12355.
48. Liu XY, Gerges N, Korshunov A, Sabha N, Khuong-Quang DA, Fontebasso AM, et al. Frequent ATRX mutations and loss of expression in adult diffuse astrocytic tumors carrying IDH1/IDH2 and TP53 mutations. Acta Neuropathol. 2012;124(5):615–25. https://doi.org/10.1007/s00401-012-1031-3.
49. Cai J, Zhang C, Zhang W, Wang G, Yao K, Wang Z, et al. ATRX, IDH1-R132H and Ki-67 immunohistochemistry as a classification scheme for astrocytic tumors. Oncoscience. 2016;3(7–8):258–65. https://doi.org/10.18632/oncoscience.317.
50. Modrek AS, Golub D, Khan T, Bready D, Prado J, Bowman C, et al. Low-grade astrocytoma mutations in IDH1, P53, and ATRX cooperate to block differentiation of human neural stem cells via repression of SOX2. Cell Rep. 2017;21(5):1267–80. https://doi.org/10.1016/j.celrep.2017.10.009.
51. Kannan K, Inagaki A, Silber J, Gorovets D, Zhang J, Kastenhuber ER, et al. Whole-exome sequencing identifies ATRX mutation as a key molecular determinant in lower-grade glioma. Oncotarget. 2012;3(10):1194–203.
52. Weber CK, Slupsky JR, Kalmes HA, Rapp UR. Active Ras induces heterodimerization of cRaf and BRaf. Cancer Res. 2001;61(9):3595–8.
53. Mizutani S, Inouye K, Koide H, Kaziro Y. Involvement of B-Raf in Ras-induced Raf-1 activation. FEBS Lett. 2001;507(3):295–8. https://doi.org/10.1016/S0014-5793(01)02992-1.
54. Wang HG, Rapp UR, Reed JC. Bcl-2 targets the protein kinase Raf-1 to mitochondria. Cell. 1996;87(4):629–38.
55. Wang HG, Takayama S, Rapp UR, Reed JC. Bcl-2 interacting protein, BAG-1, binds to and activates the kinase Raf-1. Proc Natl Acad Sci U S A. 1996;93(14):7063–8. https://doi.org/10.1073/pnas.93.14.7063.
56. Hemann MT, Lowe SW. The p53-Bcl-2 connection. Cell Death Differ. 2006;13(8):1256–9. https://doi.org/10.1038/sj.cdd.4401962.
57. Ryall S, Tabori U, Hawkins C. A comprehensive review of paediatric low-grade diffuse glioma: pathology, molecular genetics and treatment. Brain Tumor Pathol. 2017;34(2):1–11.
58. Lassaletta A, Zapotocky M, Mistry M, Ramaswamy V, Tabori U. Therapeutic and prognostic implications of BRAF V600E in pediatric low-grade gliomas. J Clin Oncol. 2017;35(25):JCO2016718726.
59. Schiffman JD, Hodgson JG, VandenBerg SR, Flaherty P, Polley MY, Yu M, et al. Oncogenic BRAF mutation with CDKN2A inactivation is characteristic of a subset of pediatric malignant astrocytomas. Cancer Res. 2010;70(2):512–9. https://doi.org/10.1158/0008-5472.CAN-09-1851.
60. Mistry M, Zhukova N, Merico D, Rakopoulos P, Krishnatry R, Shago M, et al. BRAF mutation and CDKN2A deletion define a clinically distinct subgroup of childhood secondary high-grade glioma. J Clin Oncol. 2015;33(9):1015–22. https://doi.org/10.1200/JCO.2014.58.3922.
61. Robinson JP, VanBrocklin MW, Guilbeault AR, Signorelli DL, Brandner S, Holmen SL. Activated BRAF induces gliomas in mice when combined with Ink4a/Arf loss or Akt activation. Oncogene. 2010;29(3):335–44. https://doi.org/10.1038/onc.2009.333.
62. Putlyaeva LV, Demin DE, Uvarova AN, Zinevich LS, Prokofjeva MM, Gazizova GR, et al. PTPN11 knockdown prevents changes in the expression of genes controlling cell cycle, chemotherapy resistance, and oncogene-induced senescence in human thyroid cells overexpressing BRAF V600E oncogenic protein. Biochemistry (Mosc). 2020;85(1):108–18. https://doi.org/10.1134/S0006297920010101.
63. Louis DN, Perry A, Reifenberger G, von Deimling A, Figarella-Branger D, Cavenee WK, et al. The 2016 World Health Organization classification of tumors of the central nervous system: a summary. Acta Neuropathol. 2016;131(6):803–20. https://doi.org/10.1007/s00401-016-1545-1.
64. Wellbrock C, Karasarides M, Marais R. The RAF proteins take Centre stage. Nat Rev Mol Cell Biol. 2004;5(11):875–85. https://doi.org/10.1038/nrm1498.

Publisher's Note